

NONLINER SEISMIC ANALYSIS OF STEEL ANKS UNDER HORIZONTAL AND VERTICAL BASE EXCITATIONS

Saeed SOBHAN

*PhD Candidate, School of Civil Engineering, Sharif University of Technology, Tehran, Iran.
sobhan@mehr.sharif.edu*

FayazR. ROFOOEI

*Professor, Civil Engineering Department, Sharif University of Technology, Tehran, Iran
rofooei@sharif.edu*

Keywords: Steel Tank, Seismic Behavior, Liquid-structure Interaction, Buckling, Material Plasticity

ABSTRACT

In this study the dynamic buckling behaviour of anchored cylindrical steel tanks with different aspect ratios (H/D) under tri-directional seismic input is investigated using finite element method. Two anchored steel tank with different height to diameter (H/D) ratios is considered that are subjected to tri-directional ground excitations. The effect of aspect ratio of the tank models, type of seismic ground motions and importance of simultaneous 3-directional action of seismic ground motion on the seismic behaviour and formation of elastic and plastic buckling of steel tanks is investigated. The results obtained indicate the dominant effect of the aspect ratio and the type of ground motion on seismic response of steel tanks.

INTRODUCTION

The on grade cylindrical steel tanks are the type of lifeline structures extensively used in water supply facilities, oil and gas refineries and nuclear power plants for various purposes. Extensive failures and damages observed in the on grade cylindrical steel tanks have persuaded the engineers and the researchers to investigate the seismic behavior of these structures. Housner (1963) in a pioneering work divided the hydrodynamic response of a rigid tank into two liquid impulsive and sloshing modes of vibration. The part of the liquid that vibrates with the tank's rigid body, produces the impulsive mode of response, while the rest of the liquid generates the sloshing mode and is identified with a long period of vibration.

The primary buckling modes of steel tanks wall observed in the past earthquake events are called elasto-plastic buckling and elastic buckling. The elasto-plastic failure mechanism of steel tank wall is known as the elephant foot buckling and is characterized by plastification and outward bulge of tank wall in the vicinity of its base. One type of the elastic buckling modes of steel tank is diamond shape buckling that usually occurs in the upper part of the tank wall (ALA 2001).

Experimental investigation on the buckling behavior of a small tank model constructed of Mylar A sheet, is reported by Shih and Babcock (1980). The tank model was subjected to a single horizontal harmonic and simulated seismic base excitation. They reported elastic-plastic buckling near the tank base and the elastic buckling at the top of tank wall.

Virella et al. numerically investigated the dynamic buckling of anchored steel tanks with conical roof, having aspect ratio (H/D) of 0.40, 0.63 and 0.95, using finite element method (2006). The tank models were subjected to the horizontal component of two real earthquake ground motions. Using added mass approach to model the liquid inside, they assumed that the whole liquid contributes to the impulsive response of the system. They observed two types of seismic behavior for steel tanks and determined the critical peak ground acceleration of the earthquake records causing material plasticity and elastic buckling of the tank. It was

concluded that due to a negative total pressure induced by seismic excitation, the diamond type of buckling occurred at the top of the tank shell. This conclusion verifies previous studies conducted by Nastiavas and Babcock (1987).

This study presents dynamic and buckling behavior of the on-grade cylindrical anchored steel tanks subjected to horizontal and vertical seismic ground excitations using nonlinear 3-D model of tanks. The finite element models include two anchored tank with different height to diameter (H/D) ratios under tri-directional ground excitations. Also, the influence of the aspect ratio of the tank models (H/D), type of seismic ground motions and importance of simultaneous 3- directional action of seismic ground motion on the buckling behavior of steel tanks is investigated.

TANK-LIQUID FINITE ELEMENT MODEL

In finite element model of the anchored cylindrical tank, four-node, doubly curved quadrilateral shell elements with reduced integration is used to model the surrounding wall, the bottom plate and the roof. Two-node linear beam elements are used to model the roof rafters. The liquid is modelled using eight-node brick acoustic elements. The acoustic finite elements use linear wave theory and consider the dilatational motion of the liquid.

The interaction between liquid and tank was considered using the definition "Surface tied normal contact constraint" between the interfaces of liquid and tank. This constraint is formulated based on a master-slave contact method, in which normal force is transmitted using tied normal contact between both surfaces through the simulation. The sloshing waves are considered in liquid model. Assuming the small-amplitude gravity waves on the free surface of the liquid, the boundary condition specified at free liquid surface can be presented as:

$$\frac{\partial^2 P}{\partial t^2} + g \frac{\partial P}{\partial z} = 0 \quad (1)$$

In which P is the hydrodynamic pressure at free liquid surface. Since, only anchored tanks are considered in this work, with a focus on the buckling of the cylindrical tank wall, tank models are rigidly connected to the bottom plate. The boundary conditions specified for the liquid-tank finite element model are shown in Fig. 1.

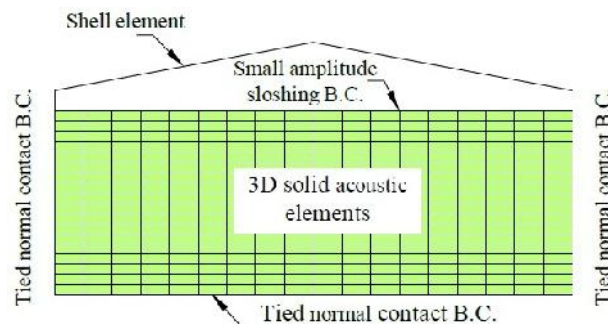


Figure 1. Boundary conditions considered for the three-dimensional liquid-tank finite element model

The tank models considered in this study are the same as the shallow tank (model A) and tall tank (model C) used by Virella et al. (2006). The height to diameter ratio (H/D) for shallow tank (model A) and tall tank (model C) are 0.40 and 0.95, respectively. The liquid level assumed for these models is 90% of the total height of the tank wall with a 10% space left as the freeboard. The thickness of tank walls that are changing with the elevation, and its geometry is shown in Fig. 2. The tanks have a cone shaped roof supported by required number of columns, ring beams and roof rafters. The one end of roof rafters or radial beams connected directly to the cylinder tank wall. Due to high axial stiffness of supporting columns, and for the sake of simplicity, these columns were replaced by roller supports.

In the finite element model, both geometric and material nonlinearities are considered. The von Mises yield criterion was defined for the plasticity of the shell element in which an elasto-plastic strain-stress curve

and steel material with yield stress of 248 MPa and Elastic modulus of 200 GPa is used. The tank content is water with density of 1000 kg/m³.

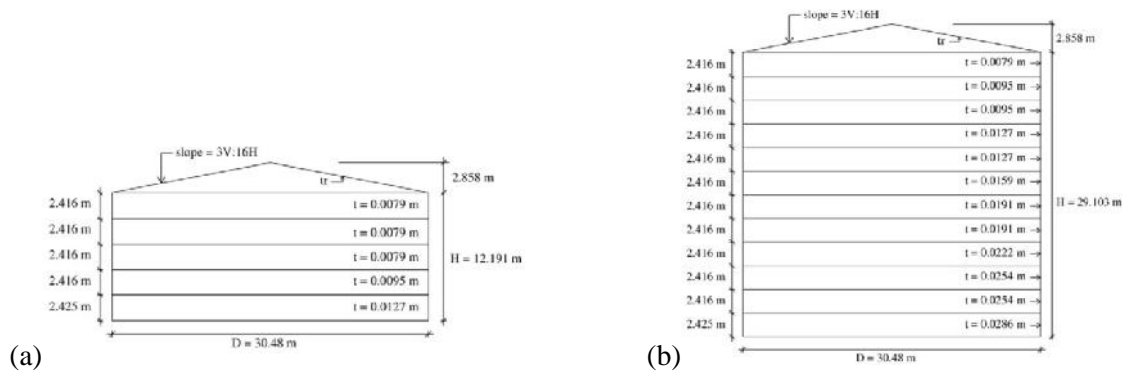


Figure 2. Geometry of the tank models: (a) Shallow tank, (b) Tall tank (Virella et al. 2006)

The analytical solutions and also numerical results reported by Virella et al. (2006) for the natural frequencies of impulsive and convective modes are used as a reference measure to evaluate the accuracy of the numerical models proposed in this study. According to API Standard 650 (2013), the fundamental impulsive mode period, in seconds, can be determined as equation (2), in SI Units:

$$T_i = C_i H_L \sqrt{\frac{D}{2000 E t_u}} \quad (2)$$

Where T_i is the fundamental impulsive periods (seconds), H_L is the liquid height (m), t_u is the equivalent uniform thickness of tank shell (mm) that are equal to 10.2 and 21.9 mm for Tanks A and C respectively, D is the tank diameter (m), E is the elastic modulus of tank material (MPa) and coefficient C_i is dependent on the H_L/D ratio and assumed as 6.9 and 6.1 for Tanks A and C, respectively. According to Eurocode 8 (2006), the natural frequencies of the first and second sloshing modes of cylindrical tank are calculated by equation (3):

$$f_n = \sqrt{g \frac{\lambda_n}{R} \tanh\left(\lambda_n \frac{H_L}{R}\right)} \quad (3)$$

In which f_n is nth natural frequency (Hz), R is radius of tank (m), λ_n is the nth positive root of Bessel function of the first order $J_1(\lambda) = 0$. The first and second positive roots of the first order Bessel function are $\lambda_1 = 1.841$ and $\lambda_2 = 5.331$ respectively. Table 1 shows the natural period of the fundamental impulsive mode, first and second convective modes determined through FE analysis for steel tanks along with those obtained from numerical and analytical solutions. The computed natural periods for steel tanks by modal analysis are in close agreement with those obtained from analytical solutions as well as the numerical results reported by Virella et al. (2006).

The Rayleigh mass proportional damping considered for the steel tank models. Assuming the modal damping ratio, ζ , of 2.0%, the mass coefficient of Rayleigh damping, β , was computed utilizing the natural frequency of the fundamental vibration mode of each liquid-tank system. According to Virella et al. (2006) the fundamental periods of tank models A and C are 0.21 and 0.30 seconds respectively. Consequently the mass proportional damping coefficients for tank models A and C are 1.20 and 0.84 respectively. The explicit time integration method is used to integrate the coupled equation of motion for tank-liquid system. This method is based on explicit central difference integration rule and benefits from the lumped and diagonal mass matrix.

Table 1. Comparison of FE results with the related analytical and numerical solutions

Tank	Fundamental impulsive period (s)				1st convective period (s)			2nd convective period (s)		
	FE	API	Virella	Diff.(%)	FE	Eurocode	Diff.(%)	FE	Eurocode	Diff.(%)
Shallow	0.213	0.205	0.212	3.90	6.094	6.174	1.30	3.365	3.395	0.88
Tall	0.306	0.297	0.300	3.03	5.653	5.754	1.76	3.364	3.393	0.85

The finite element model of model A is illustrated in Fig. 3. Since the system is subjected to tri-directional seismic ground motion, complete 3-D tank-liquid system was modelled. Also, a number of sensitivity analyses were carried out to determine the appropriate finite element mesh size with required level of accuracy of the obtained results.

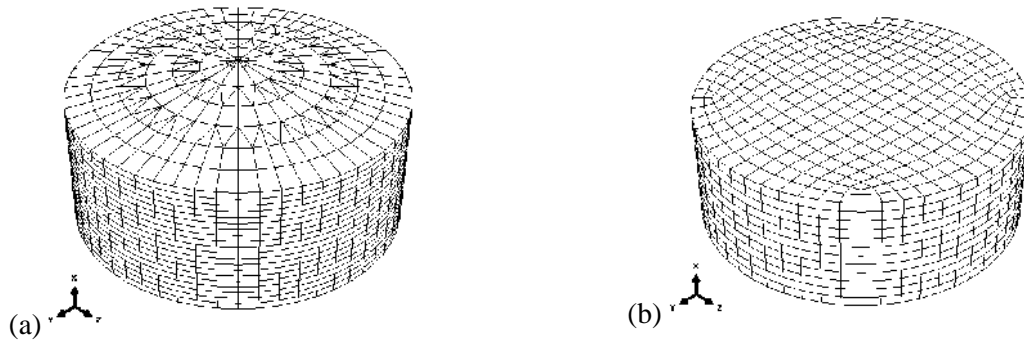


Figure 3. Finite element model of shallow tank (model A): (a) tank and (b) liquid

Four far-field and near-field pulse-like records with different frequency contents were considered in the nonlinear dynamic analysis to investigate the seismic behavior of steel tanks. According to the Fourier amplitude spectra of selected records, the Parkfield record has high frequency content, the San-Salvador and far-field Northridge records have intermediate frequency contents and the near-field Northridge record has low frequency content. All the selected accelerograms are recorded on rock or stiff soil sites. The Parkfield and Northridge (Canyon station) are far-field records, while the San-Salvador and Northridge (Rinaldi station), are considered to be near-field records. Table 2 shows the necessary information about the earthquake records used for nonlinear dynamic analyses.

Table 2. Information and parameters of seismic ground motions applied in FE analyses

No.	Earthquake	Year	Magnitude	Epicentral Distance (km)	Station	PGA (g)	PGV (cm/s)
1	Parkfield	1966	6	27	Temblor	0.27	14.5
2	San-Salvador	1986	6	4.3	CIG	0.69	80.6
3	Northridge	1994	7	26.5	Canyon	0.48	45
4	Northridge	1994	7	10.9	Rinaldi	0.87	167.3

NUMERICAL RESULTS

The incremental dynamic analyses of the tank models were carried out for the selected earthquake records scaled for several PGAs from 0.05g to 0.3g as a preliminary range of excitation intensities. The scale factor for an accelerogram computed based on the larger PGA of its two horizontal components. Then, all three components of the accelerogram are multiplied by the computed scale factor. The tank models were first subjected to gravity loads including hydrostatic and self-weight loads, before being exposed to seismic loadings. Two damage states for the tank models under seismic loading were found in this work. The material plasticity at tank wall and the elastic buckling of the tank wall were observed in liquid- tank systems.

On the other hand, the simple criteria by Budiansky and Roth (1962) that is introduced to account for the dynamic buckling load of structures, is considered in this research. The Budiansky-Roth criterion was used extensively in the literature to evaluate the critical dynamic buckling of structural systems. Based on this criterion, the dynamic analyses of structure are carried out under different level of loadings, and the specific load at which there is a significant jump in the displacement response for a small load increment is considered as the critical dynamic buckling load.

SHALLOW TANK (Model A)

The numerical results of the transient displacement response for Model A, subjected to the 1966 Parkfield accelerogram with different level of PGAs is depicted in Fig. 4(a). As it can be seen in this figure, the displacement jump occurs at the critical PGA=0.20g. The Pseudo Equilibrium Paths (PEP) for tank model

A subjected to four tri-directional earthquake records is shown in Fig. 5(a). The PEPs in Fig. 5(a) show that the tank model response has two distinct parts. For small PGAs, the plot follows an initially stable path with the slope corresponding to the initial stiffness of the tank. For higher PGAs, the slope of the curve is reduced indicating an unstable state. The two distinct parts of the curve are estimated by linear regression to form a bilinear idealization of the PEP. The intersection point of two lines corresponds to the critical PGA.

The comparison on the critical peak ground accelerations for material plasticity and elastic buckling modes for tank model A for all selected accelerograms is presented in Fig. 6(a). For model A, the material plasticity is formed at mid or bottom levels of the tank shell before or simultaneously with the occurrence of elastic buckling at the top of the cylindrical shell for all selected records. For the San-Salvador record, the material plasticity occurred in model A for a PGA=0.25g (see Fig. 7(a)), which is much less than the critical PGA=0.54g for elastic buckling mode. Therefore, shell material plasticity occurred as a damage state, before elastic buckling was formed at upper part of the tank wall. For the near-field pulse-like Northridge earthquake, in model A, the material plasticity formed at a PGA=0.25g (see Fig. 8(a)). Because of the influence of the vertical component of the near-field record, the material plasticity is observed all around the shell at the mid height of the tank shell.

TALL TANK (MODEL C)

The numerical results of transient displacement response for Model C, subjected to the 1966 Parkfield record with different level of PGAs is illustrated in Fig. 4(b). As it can be seen from this figure, the displacement jump occurs at a critical PGA=0.15g. The PEPs for the tank model C subjected to four tri-directional earthquake records is shown in Fig. 5(b). The comparison on the critical PGA for material plasticity and elastic buckling instability for tank model C for all selected records is shown in Fig. 6(b). For model C, elastic buckling is occurred at the top of the Tank shell before or simultaneously with formation of material plasticity at mid or bottom of the tank shell for all selected records. In model C, the elastic buckling mode is formed at PGA = 0.10g under the near-field Northridge earthquake, (see Fig. 7(b)), which is less than the critical PGA needed for material plasticity. Therefore, elastic buckling mode at the top of the tank wall has occurred as a damage state, before the generation of plasticity at mid height of tank shell. In model C, both the material plasticity and elastic-plastic buckling are captured at the mid height and the upper part of tank shell under the near-field Northridge earthquake record for a PGA=0.15g (see Fig. 8(b)).

The critical PGAs for material plasticity for the tank models A and C for all selected earthquake records are shown in Fig. 9(a). The comparison of the critical PGA for elastic buckling modes for the tank models A and C for all selected accelerograms is illustrated in Fig. 9(b). For both tank models A and C subjected to the Parkfield, record, elastic buckling mode and plasticity occurred at a critical PGA equal to 0.15g. Therefore, it seems that the aspect ratio (H/D) of the steel tanks under these types of earthquake records does not have significant influence on critical PGAs. For tank models A and C under near-field earthquake accelerograms (San-Salvador and Northridge), any of the critical PGA for elastic buckling mode or the critical PGA for material plasticity for tank model C is less than corresponding critical PGAs for tank model A.

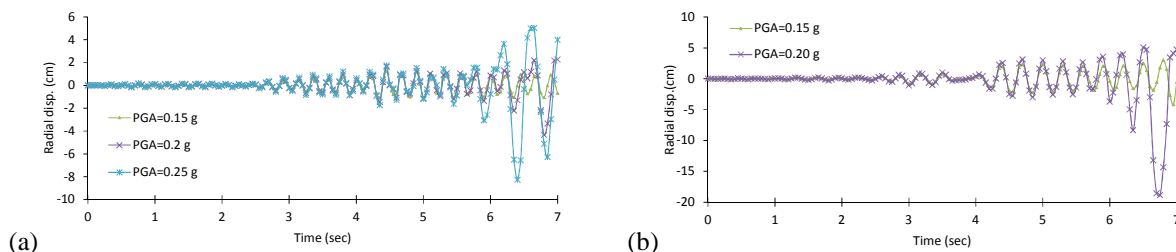


Figure 4. Time history response for (a) model A and (b) model C subjected to Parkfield record

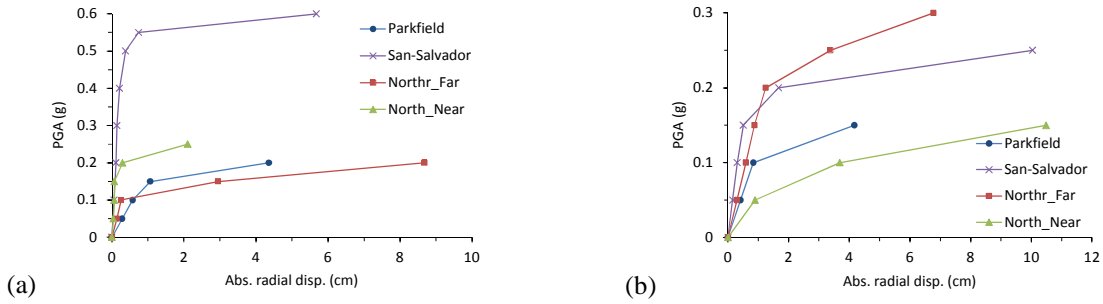


Figure 5. Pseudo Equilibrium Paths for critical node of (a) model A and (b) model C

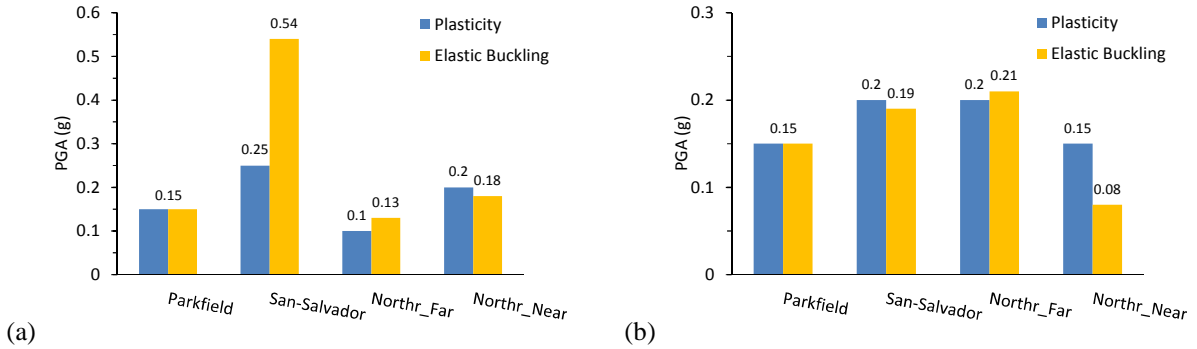


Figure 6. Critical PGAs for plastic and elastic buckling for (a) tank A and (b) tank C

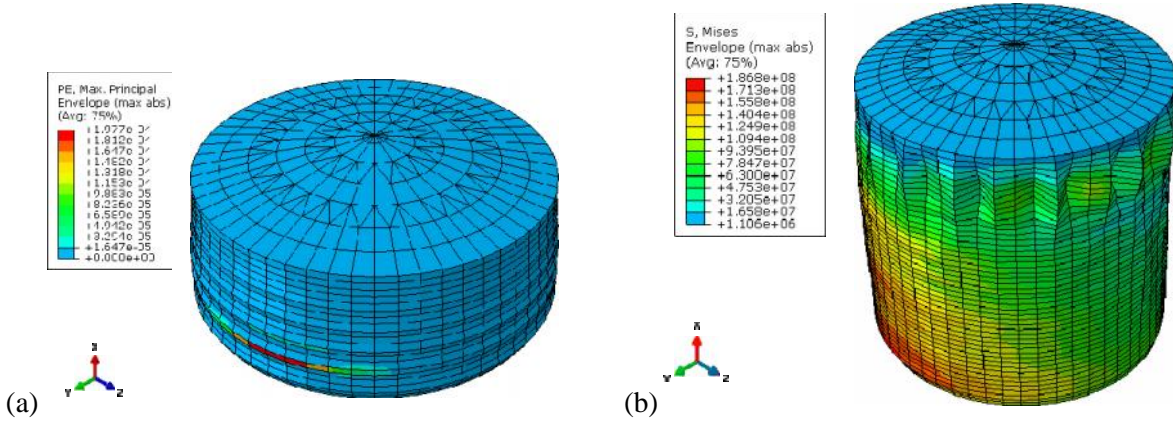


Figure 7. (a) Deformed shape and maximum plastic strains for model A subjected to the San-Salvador record with PGA=0.25g (b) Deformed shape and von Mises stresses for model C under to the San-Salvador record with PGA=0.10g

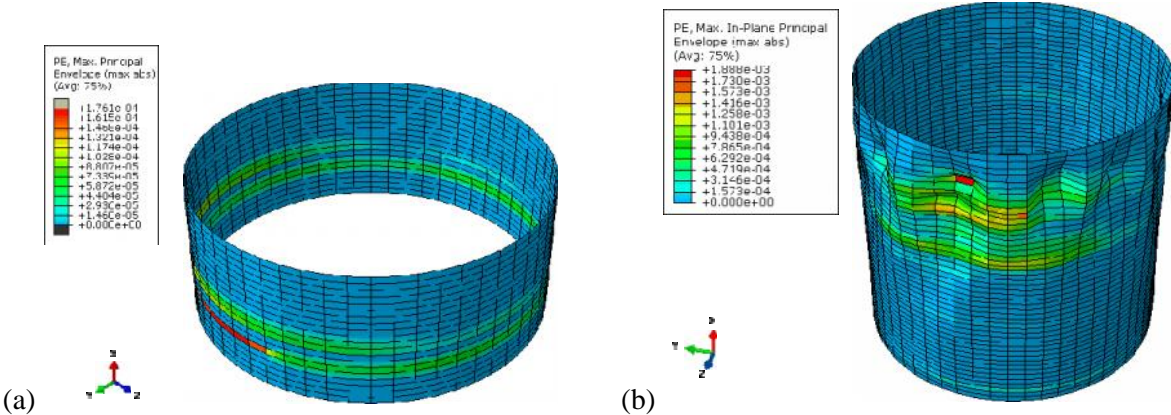


Figure 8. Maximum plastic strains of tank wall for (a) model A and (b) model C subjected to the near-field Northridge earthquake with PGA=0.20g and 0.15g respectively



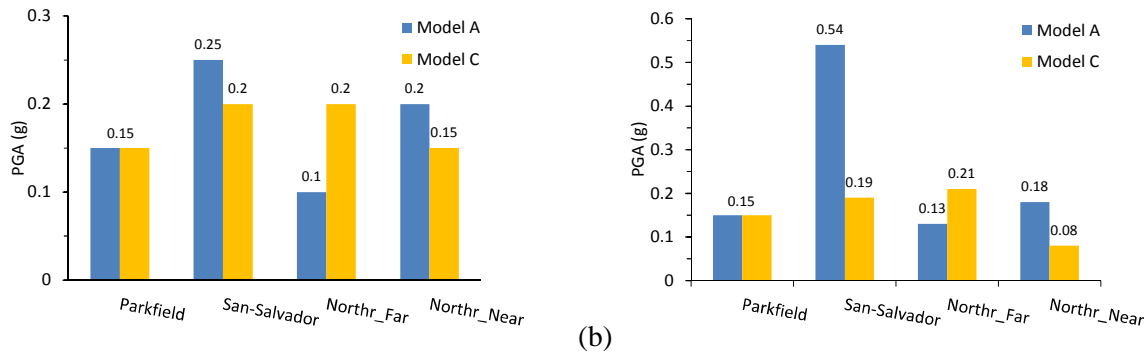


Figure 9. Critical PGAs for (a) material plasticity and (b) elastic buckling for two tank models A and C for all selected earthquake records

CONCLUSIONS

The nonlinear dynamic behavior of shallow and tall, on grade, anchored cylindrical steel liquid storage tanks is numerically evaluated using four selected tri-directionally input, near and far field earthquake records. The numerical results lead to the following conclusions:

1. For all selected accelerograms, it is observed that the plastic deformation of shallow tank ($H/D=0.40$) occurs at a PGA which is less than or equal to the PGA required for elastic buckling at the top of the tank shell.
2. For shallow tank ($H/D=0.40$) subjected to San-Salvador accelerogram, material plasticity occurs for a $PGA=0.25g$ which is much less than the critical $PGA=0.54$ for its elastic buckling mode. Therefore, shell material plasticity occurred as a damage state, before elastic buckling that was formed at upper part of the tank wall.
3. For shallow tank ($H/D=0.40$) subjected to near-field Northridge accelerogram, material plasticity has formed at mid height and all round the tank shell due to the influence of the vertical component of the near-field record.
4. For all selected accelerograms, in tall tank ($H/D=0.95$), elastic buckling has occurred at the top of the tank shell for a PGA which was less than or equal to the PGA needed for plastic behaviour of tank shell.
5. For tall tank ($H/D=0.95$) subjected to the near-field, pulse-like Northridge earthquake, both material plasticity and elastic-plastic buckling occurred for $PGA=0.15g$ at the upper part of tank shell.
6. For both shallow and tall tanks subjected to earthquake records with high frequency content (Parkfield record), elastic buckling mode and plastic behaviour occurred for critical $PGA=0.15g$. Therefore, it seems that the aspect ratio (H/D) of the steel tanks subjected to earthquake records with high frequency content does not have significant effect on critical PGAs.
7. When both tank models A and C are subjected to near-field earthquake excitations (San-Salvador and Northridge_Near), either the critical PGA for elastic buckling mode or the critical PGA for material plasticity for tank model C is less than corresponding critical PGAs for tank model A.

REFERENCES

- American Lifelines Alliance (2001) Seismic fragility formulations for water systems, ASCE, Part 1-Guideline, Part 2-Appendices
- American Petroleum Institute, API Standard 650 (2013) *Steel tanks for oil storage*, 12th Ed
- Budiansky B and Roth S (1962) Axisymmetric dynamic buckling of clamped shallow spherical shells, *NASA collected papers on stability of shell structures*, TN-1510, 597–606
- European Committee for Standardization (ECS) (2006) Design provisions for earthquake resistance of structures, Part 4 – Silos, tanks and pipelines, Eurocode 8, Brussels, Belgium
- Housner GW (1963) the dynamic behavior of water tanks, *Bulletin of the Seismological Society of America*, 53(2), 381–9
- Natsiavas S and Babcock CD (1987) Buckling at the top of a fluid-filled tank during base excitation, *ASME Journal of Pressure Vessel Technology*, 109, 374–80

Shih, CF and Babcock CD (1980) Scale Model Buckling Tests of a Fluid Filled Tank under Harmonic Excitation, Proceedings of the Pressure Vessels and Piping Conference, ASME, Preprint 80-C2/66, San Francisco

Virella JC, Godoy LA and Suarez LE (2006) Dynamic buckling of anchored steel tanks subjected to horizontal earthquake excitation, *Journal of Constructional Steel Research*, 62: 521-531

